PROCEEDINGS OF SCIENCE

$b \to s$ Penguin results from Belle II

Lucas Martel[a,*] **on behalf of the Belle II collaboration**

[a] *Université de Strasbourg, CNRS, IPHC, UMR7178, 67037, Strasbourg, France*

E-mail: lucas.martel@cern.ch

B-meson decays occurring through $b \to s$ transitions are excellent probes for new physics, as they are forbidden at tree level in the Standard Model. Thus, new physics contributions could be unequivocally identified from any deviation from their predicted branching fractions. Recent results from studies of these decays at the Belle II experiment are reported here. These results are based on a dataset corresponding to an integrated luminosity of 189 fb^{-1} and consist of measurements of $B \to K^* \ell^+ \ell^-$, $B \to J/\psi(\ell^+ \ell^-) K$ and $B \to X_s \gamma$.

20th International Conference on B-Physics at Frontier Machines (Beauty2023)
3-7 July, 2023
Clermont-Ferrand, France

*Speaker

PoS(BEAUTY2023)008

1. Introduction

Amongst the B-meson decays studied to search for new physics, the flavour-changing neutral current $b \to s$ quark transitions are of particular interest, since they are forbidden at tree level in the Standard Model and only occur through loop amplitudes. Several models expect modifications of the branching fractions for these processes, coming from new physics contributions. Any deviation from the branching fraction values predicted by theory would thus be a clear sign of these new physics controbutions.

The Belle II experiment[1] consists in the Belle II detector located at the SuperKEKB [2] collider in Tsukuba, Japan. SuperKEKB produces asymmetric e^+e^- collisions at the $\Upsilon(4S)$ resonance and holds the world record for the highest instantaneous luminosity (4.7×10^{34} cm^{-2}s^{-1}). Since the beginning of the data collection in early 2019, Belle II has recorded a dataset corresponding to an integrated luminosity of 362 fb^{-1} at the $\Upsilon(4S)$ energy, and is set to record 50 ab^{-1} by the end of its lifetime. The studies presented here are all based on a dataset corresponding to 189 fb^{-1}, collected between 2019 and 2021.

2. Experimental results

2.1 Measurement of $B \to K^*\ell^+\ell^-$

This section reports the measurement of the branching fractions of the rare decays $B \to K^*(892)\ell^+\ell^-$, with $\ell = e, \mu$. These decays exhibit small branching fraction values, at the order of 10^{-6}, making their observation challenging. Charged final state particle candidates (pions, kaons and leptons) are reconstructed from Belle II detector information. In addition, neutral pion candidates are reconstructed from pairs of photons and K^0_S are reconstructed from pairs of opposite charge pions. The K^* candidates are reconstructed in the $K^{*+}(892) \to K^0_S\pi^+$, $K^{*+}(892) \to K^+\pi^0$ and $K^{*0}(892) \to K^+\pi^-$ channels. B-meson candidates are then reconstructed in the $B \to K^*(892)\ell^+\ell^-$ channels.

In order to limit background contamination, the di-lepton mass ranges corresponding to γ, J/ψ and $\psi(2S)$ are vetoed. Additionaly, a boosted decision tree is used to suppress remaining backgrounds. The signal yields are then extracted from a simultaneous fit to the beam-energy constrained mass M_{bc} and the energy difference ΔE defined as:

$$M_{bc} \equiv \sqrt{\left(\frac{\sqrt{s}}{2}\right)^2 - p^{*2}_B}, \qquad \Delta E \equiv E^*_B - \frac{\sqrt{s}}{2}, \tag{1}$$

with $\sqrt{s}$ the collision energy in the center of mass system (CMS), and E^*_B and p^*_B are respectively the energy and momentum of the B-meson candidate in the CMS. The results of the fit can be seen in Figure 1.

From this, the values of the branching fractions are computed, giving:

$$\begin{aligned} \mathcal{B}(B \to K^*(892)\mu^+\mu^-) &= 1.19 \pm 0.31\ (\text{stat})\ ^{+0.08}_{-0.07}\ (\text{syst})\ , \\ \mathcal{B}(B \to K^*(892)e^+e^-) &= 1.42 \pm 0.48\ (\text{stat})\ \pm 0.09\ (\text{syst})\ , \end{aligned} \tag{2}$$

which show good agreement with the world average[5]. In addition, comparing the two values shows that Belle II reaches similar perfornances for the electron and muon modes.

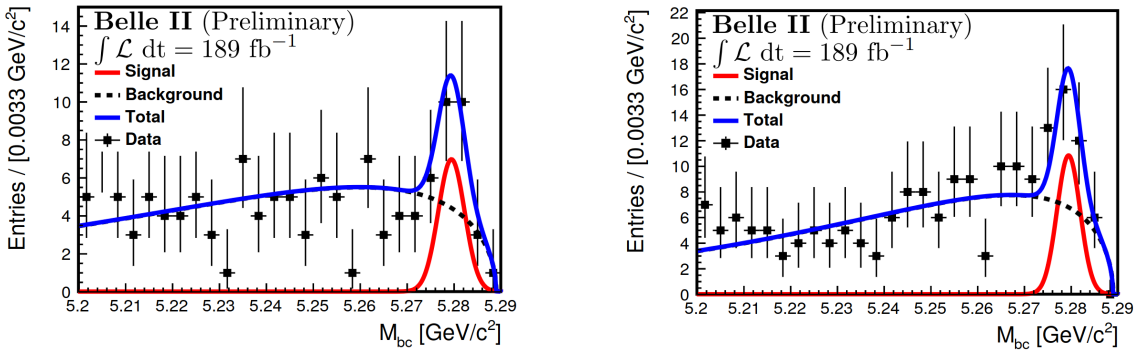

(a) (b)

Figure 1: Beam-energy constrained mass for the $B^+ \to K^{*0}(892)e^+e^-$ (a) and $B^+ \to K^{*0}(892)\mu^+\mu^-$ (b) candidates for data (black dots) and the fit prediction (blue curve). The two components of the fit are shown: signal modeled with a Gaussian (red curve) and background modeled with an ARGUS shape [3] (dashed black curve). Taken from [4]

.

2.2 Lepton-flavour universality in $B \to J/\psi(\ell^+\ell^-)K$

This section reports the measurement of the $R_K(J/\psi)$ ratio, defined as:

$$R_K(J/\psi) \equiv \frac{\mathcal{B}(B \to J/\psi(\mu^+\mu^-)K)}{\mathcal{B}(B \to J/\psi(e^+e^-)K)}. \tag{3}$$

Even though the $B \to J/\psi(\ell^+\ell^-)K$ decays occur through a favoured $b \to c$ transition, they are discussed here as control channels for the measurement of the ratio R_K:

$$R_K \equiv \frac{\mathcal{B}(B \to K\mu^+\mu^-)}{\mathcal{B}(B \to Ke^+e^-)}. \tag{4}$$

Here, the measurement of $R_K(J/\psi)$ is performed in the $B^+ \to J/\psi K^+$ and $B^0 \to J/\psi K^0_S$ channels. J/ψ and K^0_S candidates are reconstructed from their decay products (pairs of opposite sign leptons and pions, respectively), with requirements on their invariant mass in order to suppress background contributions. B-meson candidates are then reconstructed from a J/ψ and kaon candidate.

The signal yields are then extracted from a simultaneous fit to M_{bc} and ΔE as can be seen in Figure 2 for the $B^+ \to J/\psi(\mu^+\mu^-)K^+$ mode. From this, the $R_K(J/\psi)$ values are computed:

$$\begin{aligned} R_{K^+}(J/\psi) &= 1.009 \pm 0.022 \pm 0.008 \\ R_{K^0}(J/\psi) &= 1.042 \pm 0.042 \pm 0.008 \end{aligned} \tag{5}$$

The measured ratios are in agreement with unity (expected in the Standard Model) and their associated uncertainties are largely dominated by the statistical components. In addition, the systematic uncertainty associated to the ratios is better than the ones published by Belle[7].

2.3 Fully inclusive measurement of $B \to X_s\gamma$

The measurement of the branching fraction of the inclusive $B \to X_s\gamma$ decays is reported here. In order to suppress most background, events are reconstructed as $e^+e^- \to B_{sig}B_{tag}$, with

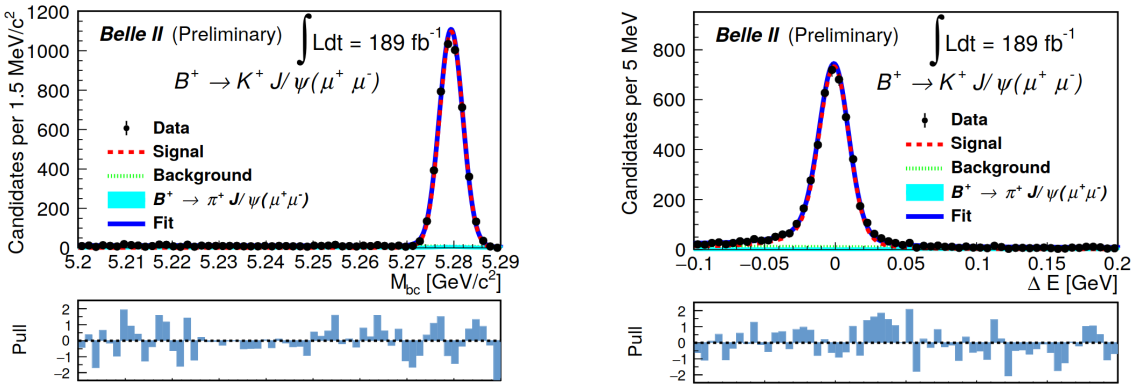

(a) (b)

Figure 2: Beam-energy constrained mass (a) and energy difference (b) for the $B^+ \to K^+\mu^+\mu^-$ candidates for data (black dots) and the fit prediction (blue curve). The components of the fit are shown: signal (red curve), background from $B^+ \to J/\psi(\mu^+\mu^-)\pi^+$ (filled blue histogram) and the remaining background (dashed green curve). Taken from [6].

E_γ^B threshold [GeV]	$\mathcal{B}(B \to X_s\gamma)$ [10^{-4}]	Experiment
1.8	$3.54 \pm 0.78 \pm 0.83$	Belle II [9]
2.0	$3.06 \pm 0.56 \pm 0.47$	Belle II [9]
1.6	3.49 ± 0.19	World average [5]

Table 1: Branching fraction values of the inclusive $B \to X_s\gamma$ decay measured in Belle II for two threshold of the photon energy E_γ^B. The first (second) quoted uncertainty corresponds to the statistical (systematic component). The world average for another E_γ^B threshold is also given.

$B_{sig} \to X_s\gamma$, and B_{tag} the partner B-meson. This method is called hadronic B-tagging. This measurement is performed by using the `FEI` algrithm[8] developped by the Belle II collaboration, which uses tracks and calorimeter energy deposits to reconstruct the most probable B_{tag} decay in a list of $\sim$ 30 fully hadronic decay modes.

After reconstructing the B_{tag}, the most energetic remaining photon is identified as the signal photon. Background contributions from $\pi^0 \to \gamma\gamma$ and $\eta \to \gamma\gamma$ are suppressed with a multivariate classifier using information from calorimeter energy deposits. In addition, background coming from $e^+e^- \to q\bar{q}$ (with q is a u, d, c or s quark) is suppressed with an additional classifier trained with kinematic features of the event.

A fit to M_{bc} is then performed in bins of E_γ^B, the photon energy in the signal B-meson frame , as shown in Figure 3(a), providing yields corresponding to $B \to X_s\gamma$, as well as other B-meson decays, which are estimated using simulations as shown in Figure 3(b).

Table 1 shows the branching fraction values measured for different E_γ^B thresholds. The results are in agreement with the world average and competitive with the previous measurement performed by BaBar[10] using a similar technique and sample size. Here, the systematic component of the uncertainties is mainly due to background mis-modelling.

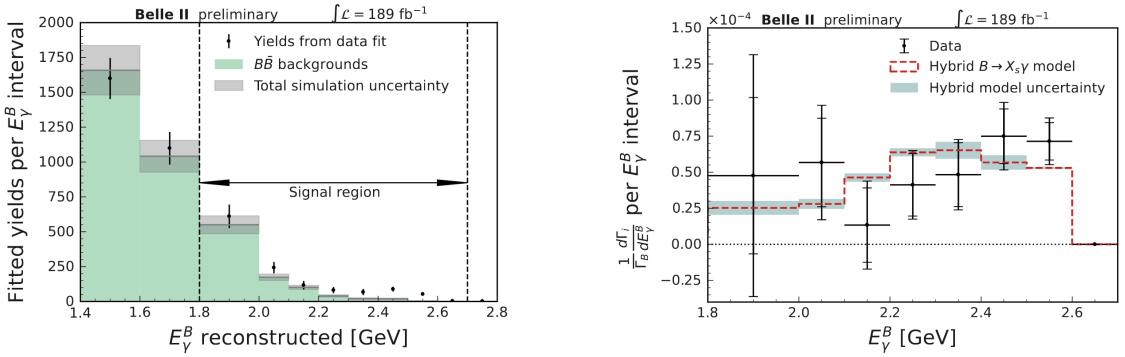

(a) (b)

Figure 3: Fitted yields of $B\bar{B}$ events (a) and partial width of the inclusive $B \to X_s\gamma$ decay (b) in intervals of E_γ^B. In (a) the yields from the fit to data are shown with black dots, while the filled green histogram corresponds to the contribution from $B\bar{B}$ background. The filled grey histogram shows the uncertainty associated to the simulation. The excess seen in data with respects to the $B\bar{B}$ background corresponds to the $B \to X_s\gamma$ contribution. In (b) the black dots correspond to branching fraction values measured in data with the inner (outer) error bars showing the statistical (total) uncertainty associated to them. The dashed red histogram shows the prediction of the signal model while the filled grey histogram corresponds to its associated uncertainty. Taken from [9].

3. Summary

Several Belle II results on $b \to s$ penguin (and $b \to c$) transitions have been presented here. The Belle II measurement of the branching fractions for the decays $B \to K^*(892)\ell^+\ell^-$, which is the first step towards the measurement of the R_K ratios, show an agreement with the world averages. The measurement of the branching fractions for the $B \to J/\psi(\ell^+\ell^-)K$ decays as well as the $R_K(J/\psi)$ value are also reported, showing an agreement with world averages and theory predictions while displaying the experiment's ability to perform good and similar identification of electrons and muons. Finally, the first measurement of the inclusive $b \to s\gamma$ transition using hadornic B-tagging by the Belle II experiment is also reported, providing a measurement competitive with only previous hadronic B-tagging analysis by BaBar.

References

[1] Belle II collaboration, *Belle II Technical Design Report*, 1011.0352.

[2] K.Akai et al., *SuperKEKB collider*, Nucl. Instrum. Meth. A 907, 2018.

[3] ARGUS collaboration, *Search for hadronic $b \to u$ decays*, Phys.Lett.B 241 (1990).

[4] Belle II collaboration, *Measurement of the branching fraction for the decay $B \to K^* \ell^+ \ell^-$ at Belle II*, 2206.05946.

[5] Particle Data Group, *Review of Particle Physics*, PTEP **2022** (2022) 083C01.

[6] Belle II collaboration, *Measurements of the branching fraction, isospin asymmetry, and lepton-universality ratio in $B \to J/\psi K$ decays at Belle II*, 2207.11275.

[7] Belle collaboration, *Test of lepton flavor universality and search for lepton flavor violation in $B \to K\ell\ell$ decays*, JHEP **03** (2021) 105 [1908.01848].

[8] T.Keck et al., *The Full Event Interpretation*, Comput. Softw. Big Sci. **3** (2019) 6 [1807.08680].

[9] Belle II collaboration, *Measurement of the photon-energy spectrum in inclusive $B \to X_s\gamma$ decays identified using hadronic decays of the recoil $\bar{B}$ meson in 2019-2021 Belle II data*, 2210.10220.

[10] BaBar collaboration, *Measurement of the $B \to X_s\gamma$ branching fraction and photon energy spectrum using the recoil method*, JHEP **03** (2021) 105 [1908.01848].